Water-Silanol Interactions on the Amorphous Silica Surface: a dispersion-corrected DFT Investigation

Youssef Berro[a,b], *Michael Badawi*[a,*] *Fouad El Haj Hassan*[b], *Mounir Kassir*[b], *and Frederik Tielens*[c,*]

[a] Laboratoire de Physique et Chimie Théoriques LPCT – UMR CNRS 7019, Université de Lorraine, Vandœuvre-lès-Nancy, France.

[b] Plateforme de Recherche et d'Analyse en Sciences de l'Environnement PRASE, Université Libanaise, Hadath, Liban.

[c] General Chemistry (ALGC), Vrije Universiteit Brussel (Free University Brussels-VUB), Pleinlaan 2, 1050 Brussel, Belgium.

*corresponding authors: michael.badawi@univ-lorraine.fr; frederik.tielens@vub.be

ABSTRACT

Interpreting the interaction between the amorphous silica surface and water is a key step to understand its physicochemical properties. However, due to the flexibility of the structure and the distribution of types and geometries of the silanols one can obtain a broad range of interaction energies, as was already shown in former studies. This time we were able to investigate the distribution of silanols in relation with the calculated interaction energies, and thus designate those different silanols sites. Different dispersion-correction PBE-D (PBE + D2, D3, D3-BJ, TS, TS-HI, MBD, and FI-MBD) and meta-GGA SCAN methods has been used to quantify the interactions between water and defined silanols sites of the surface. All the methods give similar interaction energies, showing equivalent performances of SCAN and PBE-D methods to describe week interactions in our system. Following various routes, we identified a protocol of calculation in order to compute the interaction energies more accurately, taking into consideration the van der Waals (vdW) forces. Once different silanols are correctly described within the calculation level, it is clear that the geometry and environment determine its chemistry. Furthermore, the possible deformation of the silica surface affected by the water interaction is studied. The quantification of the interaction energies is important in order to correctly scale the results and confront with the experiments. With this information in mind, one can think about synthesis techniques that modify the silanols distribution of the silica surface in a way to tune its hydrophobicity and acidity.

Keywords

dispersion-corrected DFT; amorphous silica; silanol defects; water interaction; SCAN

1. INTRODUCTION

Being one of the most famous materials used in adsorption and catalysis applications due to its structural properties [1–6], the amorphous silica (silicon dioxide) has been investigated using density functional theory (DFT) calculations during the last decade [7–10]. The physico-chemical properties of the amorphous silica are ruled by the presence of silanol groups [11,12], which are characteristic defects in the bulk and at the surface or interface of the finite particles. Due to the intrinsic properties of the amorphous structure of silica, different types of silanol groups can be distinguished which geometrical parameters are spread over a distribution function depending of the origin and synthesis protocol followed. This statistical feature makes it difficult to assign one property to one specific type of silanol group. The prediction of macroscopic or global properties such as hydrophobicity, or acidity is also challenged by this statistical distribution of silanol groups, because one type of silanol groups can show opposite properties depending on the local environment and surface concentration [13–15]. In order to understand the evolution of the chemistry within one type of silanol group over the property range (mainly ruled by the local geometry), the silanol group interactions should be accurately described. It is the combination of the accurately described properties of the silanol groups over a statistical distribution that might enable the overall description of the investigated amorphous silica.

The construction of models is in the case of amorphous silica the most delicate milestone [16–21]. In recent years, some of us specialized in combining the amorphicity, size and periodicity in one model, with the aim to perform DFT calculations on amorphous silica [14,21–32], and in particular to investigate its hydration and acidity [25,29,31]. The chemistry of the silanol groups at the amorphous silica surface is dependent on: a) the coverage, b) the type of silanol (isolated, vicinal, geminal, and in nests), and c) the inter-molecular interactions between

the silanol groups (mainly H-bonds) [14,33,34]. The accurate description of H-bonds in quantum chemistry is not new and present a recurrent problem [35,36]. In 2006, van der Wijst *et al.*[37] compared the performance of different popular density functionals (B3LYP, BLYP, BP86, mPW, OPBE, PBE, PW91) for describing the geometry and stability of hydrogen bonds in DNA base pairs. They showed that results obtained from BP86 and PW91 were consistent with ab initio and experimental results, while B3LYP functional underestimates the strengths and overestimate the distances of hydrogen bonds. In contrast, the B3LYP functional overestimates the strength of hydrogen bonds in the case of clusters of methanol when using insufficiently complete basis set [38], meaning that the capability of the DFT methods to determine the strength of H-bonds can be assessed with the used basis sets. Some years later, Grimme et al. [39] evaluated the performance of 17 dispersion corrected density functional methods on the new S66 and S66x8 benchmark sets for non-covalent interactions showing that double-hybrid functionals are the most robust and accurate methods.

Nowadays, within the periodic DFT framework [40], different methods are able to tackle this problem ranging from adapted functional to empiric London-dispersion corrections [41–43]. Indeed, the last decade has witnessed tremendous effort in the development of various correction methods to account for the missing London dispersion interactions in conventional Kohn-Sham DFT calculations [44]. Two types of approaches are mainly used. One can use specific non-local correlation functionals that approximately account for dispersion interactions, as originally developed by Dion et al. [45] and improved by other groups [46,47]. However, due to the relatively high cost of calculation, we decided to focus in the present work on the second approach that considers the additive correction schemes to include dispersion interactions [48]. According to this approach, different methods have been developed during the few precedent

years, among them the D2 [44,49,50], D3 [51], D3-BJ [52], TS [53,54], TS-HI [55,56], MBD [57–59], and FI-MBD [60] methods that will be described in the computational details section. The performances of these dispersion-corrected methods will be compared with the recently developed meta-GGA SCAN functional, which should correctly describe hydrogen bonds [61]. This method, at almost GGA cost, matches or improves on the accuracy of expensive hybrid functional when used to predict geometries and energies of diversely bonded molecules and materials (including covalent, ionic, metallic, hydrogen, and van der Waals bonds) [61].

In the present paper, we study the interaction between the amorphous silica and water, as a probe for the silanol chemistry, using the DFT-D toolbox in order to describe as accurate as possible the different types of silanol groups (isolated, vicinal, geminal, and in nests) independently. This will help to the understanding of the complex amorphous silica-water interface investigated since a decade [24,25].

2. COMPUTATIONAL DETAILS

2.1 Calculation settings

The Vienna Ab initio Simulation Package (VASP) software has been employed to perform DFT periodic calculations [62,63]. Perdew Burke Ernzerhof (PBE) [64] semi-local exchange-correlation functional is chosen, and electronic wave functions are expanded into plane waves with a cut-off energy of 450 eV. Electron-ion interactions have been described using the projected-augmented-wave (PAW) method [65]. Kohn-Sham equations are solved self-consistently until an energy difference of 10^{-6} eV is reached [66]. Atomic positions relaxation has been done until all forces become smaller than 0.01 eV/ Å per atom. The Γ-point is used in the Brillouin-zone integration.

London dispersion interactions have been taken into account using several correction additive schemes to the PBE calculations. All these corrective methods provide an E_{disp} term to be added to the Kohn Sham energy and are available now in the VASP package [50,54–56,59,60]. These methods include pairwise additive correction schemes of Grimme [44,49–52] in which the C_6 coefficients are available in literature (semi-empirical D2 [49] or corrected depending on the coordination number D3 [51]). In the D3-BJ version, the damping function has been improved [52]. Tkatchenko and Scheffler (TS) have developed another approach based on the determination of C_6 on the fly, depending on the chemical environment [53,54]. The Tkatchenko-Scheffler scheme with iterative Hirshfeld partitioning, TS/HI, is later developed and implemented in VASP by Bučko and co-workers [55,56] and proved to describe more accurately dispersion interactions in both covalent and ionic systems [43,67]. The more sophisticated non-additive many-body variants of the TS scheme based on the adiabatic connection fluctuation-dissipation (ACFD) theorem [57,58], without (MBD) [59] and with (MBD-FI) [60] taking account of the ionicity effect, are discovered recently. The meta-GGA SCAN (Strongly Constrained and Appropriately Normed) functional obeys all 17 known exact constraints that a meta-GGA can and it is nearly exact for a set of appropriate norms including rare-gas atoms and non-bonded interactions, which make it more accurate to describe weak interactions [61,68].

2.2 Structural model

The amorphous silica model structure developed and studied by Tielens and his co-workers [21], which present a silanol density of 5.8 OH/nm^2 has been employed. The surface unit cell parameters are a = 12.77 Å, b = 17.64 Å, c = 25.17 Å (including 15 Å of vacuum) and it is composed of 27 Si, 67 O, and 26 H atoms. **Figure 1** shows, from different views, the structure of the amorphous silica model and the types of studied silanols within. Silanol sites present on the

amorphous silica surface were described based on their type and the surrounding environment. Six sites were studied, (i) the isolated site, (ii) the geminal site, (iii) the vicinal site, (iv) the gem-vic site, (v) the nest-1 site, and (vi) the nest-2 site.

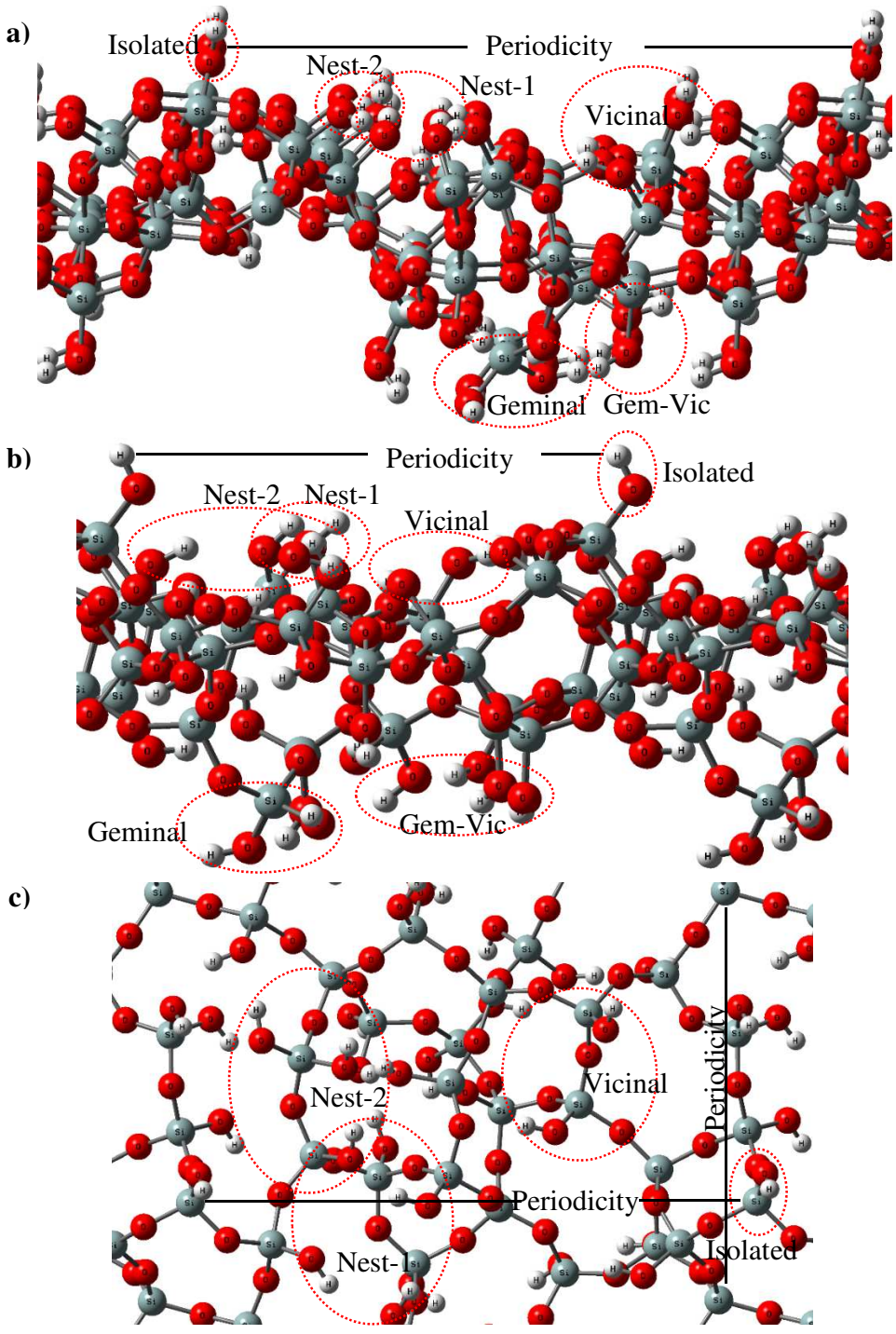

Figure 1. *Different silanols sites of the amorphous silica model from various views: a) side view-1, b) side view-2, and c) top view (oxygen atom sphere in red, silica in grey, hydrogen in white).*

2.3 Adsorption model

Figure 2 shows the various methods and starting geometries used to perform the calculations. Starting from a first initial geometry ("fromGeom0"), we relaxed the geometry of all systems (silica surface, water molecule, silica and water) using PBE functional or different dispersion-corrected PBE methods (PBE + D2, D3, D3-BJ, TS, TS-HI, MBD, FI-MBD). Using the new geometry obtained after the relaxation using the PBE method ("fromPBE") we performed single point dispersion-corrected PBE, dispersion-corrected PBE and meta-GGA SCAN geometry relaxations. As well, using the geometry obtained after the relaxation using PBE+D2 ("fromD2"), we performed dispersion-corrected PBE single point and geometry relaxation calculations.

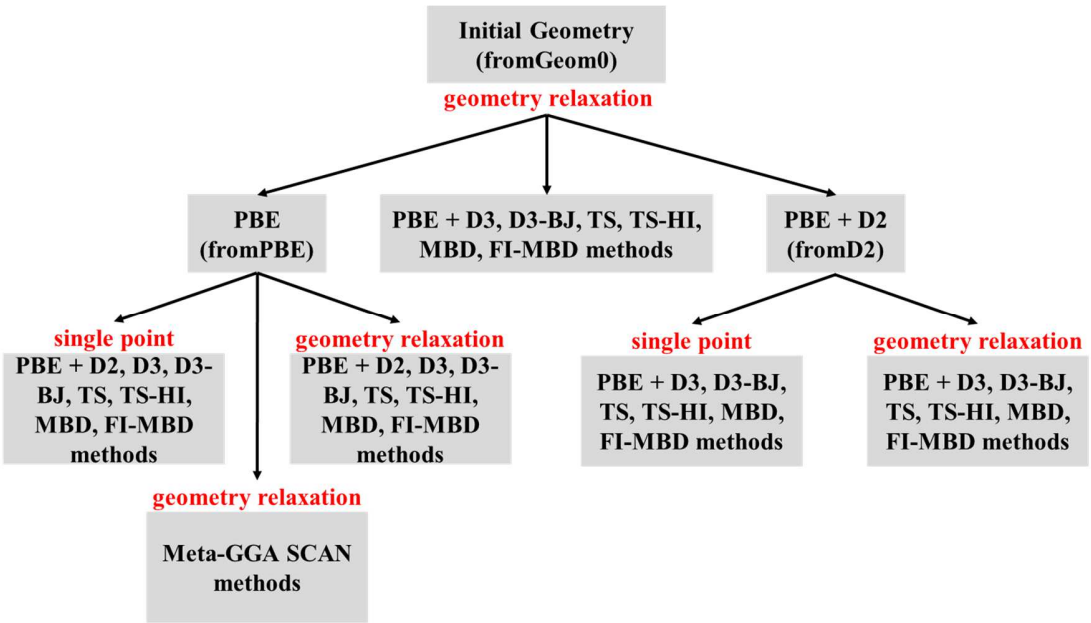

Figure 2. *Scheme showing the various methods* (GGA PBE, *dispersion-corrected PBE, and meta-GGA SCAN*) *and starting geometries used to perform single point and relaxation calculations.*

For each method, the interaction energy between one type of silanol and water molecule has been determined through several sets of DFT calculations that allow to obtain the energy of pure silica surface E_{Sil}, the energy of isolated water molecule in the gaseous phase E_{water}, and the energy of the system (water molecule on silica surface) $E_{Sil-water}$. This energy, E_{int}, having a positive value corresponding to an exothermic process is determined as follows:

$$E_{int} = E_{Sil} + E_{water} - E_{Sil-water} \qquad (1)$$

In the case of dispersion-corrected PBE methods, the interaction energy can be described as the sum of the PBE (E_{PBE}) and dispersion (E_{disp}) energies.

$$E_{int} = E_{PBE} + E_{disp} \qquad (2)$$

3. RESULTS AND DISCUSSIONS

3.1 Protocol of relaxation

The interaction energies, between water and silanols, and their relative PBE and dispersion contributions have been evaluated, they are computed using DFT+D calculations over each site of the amorphous surface using different dispersion-correction methods. The integration of the vdW forces effect using those correction methods is made via three different routes (**Figure 2**). The first route is called "fromGeom0", in which the non-corrected PBE, the corrected D2, D3, D3-BJ, TS, TS-HI, MBD, and FI-MBD methods were applied directly for a randomly placed water molecule over the selected site. The second route is called "fromPBE", in which firstly a geometry relaxation of the system for a randomly placed water molecule on the chosen site is done using PBE calculations, and then the dispersion-correction methods are added to perform

new corrected relaxation on the PBE pre-relaxed configuration. The third route is called "fromD2", which is similar to the second route but with the relaxation using various correction methods (D3, D3-BJ, TS, TS-HI, MBD, FI-MBD) of the PBE+D2 pre-relaxed geometry. As well, single point dispersion-corrected PBE calculations were performed on those two pre-relaxed configuration ("fromPBE" and "fromD2"). All those calculations aim to define a protocol of calculation in order to include the effect of the dispersion forces using the most accurate method keeping also in mind the calculation time. For the isolated, vicinal, geminal, and nest-1 silanols, a full relaxation calculation always lead to the same minima for a given level of theory, whatever the starting geometry, *see Tables S1 to S4* in ***Supplementary Material.*** However, the interaction energies over the Gem-Vic (**Table 1**) and the nest-2 (**Table 2**) sites are affected by the calculation procedure. The accuracy of the calculation procedure is assessed by comparing the total interaction energies following various routes, and by comparing the PBE contribution part of the interaction energy for dispersion-corrected calculation, with the non-corrected PBE interaction energy. These two criteria can give us an information about the reliability of the obtained results following the various method and routes in order to define a protocol of calculation that can be used to other similar systems.

Table 1. *Water interaction energies (PBE and dispersion contribution) over the gem-vic site of the amorphous surface obtained by single point and geometry relaxation calculations using various procedure routes (different starting geometries and correction methods).*

E_{int} (E_{PBE}/E_{disp}) (kJ/mol)	**PBE**	**PBE +D2**	**PBE +D3**	**PBE+D3-BJ**	**PBE +TS**	**PBE+TS-HI**	**PBE +MBD**	**PBE+FI-MBD**
fromGeom0 *relaxation*	58	64 (46/18)	69 (57/12)	70 (57/13)	62 (49/13)	59 (50/9)	62 (48/14)	59 (49/10)
fromPBE *single point*	*	72 (57/15)	69 (58/11)	71 (59/12)	81 (67/14)	83 (71/12)	93 (71/22)	91 (71/20)
fromPBE *relaxation*	*	72 (58/14)	69 (58/11)	71 (58/13)	70 (58/12)	67 (57/10)	72 (57/15)	69 (58/11)
fromD2 *single point*	*	*	60 (47/13)	61 (47/14)	61 (47/14)	56 (46/10)	61 (46/15)	59 (46/13)
fromD2 *relaxation*	*	*	61 (48/13)	61 (47/14)	61 (48/13)	57 (47/10)	62 (47/15)	60 (47/13)

Table 2. *Water interaction energies (PBE and dispersion contribution) over the nest-2 site of the amorphous surface obtained by single point and geometry relaxation calculations using various procedure routes (different starting geometries and correction methods).*

E_{int} (E_{PBE}/E_{disp}) (kJ/mol)	**PBE**	**PBE +D2**	**PBE +D3**	**PBE+ D3-BJ**	**PBE +TS**	**PBE+TS -HI**	**PBE +MBD**	**PBE+FI -MBD**
fromGeom0 *relaxation*	74	61 (49/12)	93 (77/16)	95 (77/18)	96 (77/19)	88 (76/12)	90 (74/16)	93 (76/17)
fromPBE *single point*	*	97 (76/21)	88 (77/11)	88 (79/9)	99 (87/12)	106 (92/14)	116 (91/25)	115 (92/23)
fromPBE *relaxation*	*	97 (77/20)	93 (76/17)	94 (75/19)	96 (74/22)	88 (76/12)	95 (75/20)	93 (76/17)
fromD2 *single point*	*	*	60 (49/11)	59 (49/10)	61 (49/12)	56 (50/6)	60 (49/11)	58 (49/9)
fromD2 *relaxation*	*	*	61 (52/9)	60 (50/10)	95 (77/18)	88 (78/10)	60 (50/10)	58 (50/8)

Table 1 and **Table 2** shows that the best route to follow, in the search for the optimal calculation procedure, is to perform firstly a non-corrected PBE calculation to relax the geometry of a randomly placed water molecule over the site of the amorphous silica surface. Then relaxing again the "fromPBE" configuration using DFT+D calculation by adding one of the dispersion-correction methods. Using this procedure, we can always attain the most stable state of the system, as we obtain the minimal total energy of the system which is inversely proportional to the total interaction energy (as the total energy of silica surface and water are not highly affected by the method or route used). In fact, when relaxing directly the "fromGeom0" using DFT+D, one can underestimate the PBE contribution (e.g. in **Table 1**, when using PBE + D2, TS, TS-HI, MBD, and FI-MBD to relax "fromGeom0" system). Therefore, we performed single point and relaxation dispersion-corrected calculations on the pre-relaxed non-corrected configuration ("fromPBE") and on the pre-relaxed D2-corrected configuration ("fromD2") aiming to attain a better accuracy with less computational costs. However, single point calculations of the pre-relaxed "fromPBE" configuration does not allow reaching the best ground state energy of the system, which implicate a misestimating of the PBE part (e.g. in **Table 1**, when performing single point calculations for the "fromPBE" configuration using the PBE + TS, TS-HI, MBD, and FI-MBD methods). When performing geometry relaxation calculations on the pre-relaxed "fromD2" configuration using more sophisticated dispersion-correction methods, the structure can be trapped in the local energetic minimum state found using the D2 method (e.g. in **Table 2**, when using PBE + D3, D3-BJ, MBD, and FI-MBD to relax "fromD2" system). An additional evidence of this observation is that performing single point calculations using those vdW methods (D3, D3-BJ, MBD, FI-MBD) of "fromD2" configuration give the same interaction energies as the full relaxations. This was not the case for "fromPBE" full relaxations, meaning

that the system always get out from the local minima (e.g. in **Table 1**, single point and full relaxation of "fromPBE" configuration using PBE+MBD method).

It is noticeable that by using the pre-relaxed "fromPBE" system, all dispersion-correction methods (from the simple D2 to the more sophisticated FI-MBD) proved to possess the ability to estimate the interaction energy within 5%, which can be considered as the standard error of the DFT calculation itself. However, the D2 method tends to give higher interaction energies than other methods and the TS-HI method tends to underestimate those energies. Finally, from an accuracy/cost point of view, applying D2 on a pre-relaxed "fromPBE" system can be sufficient to calculate the interaction energy of the water molecule on the selected site of the amorphous silica surface. To summarize, relax the pre-relaxed "fromPBE" configuration appears as the best option to reach the best local minima of the potential energy surface and describe more accurately the interaction between water and the different silanols types.

3.2 Analysis of the water interaction over different sites of the amorphous silica

The interaction (electrostatic PBE and dispersion contribution) energies of water on selected sites of the silica surface computed by relaxing the pre-relaxed "fromPBE" system using various dispersion-correction PBE methods (PBE + D2, D3, D3-BJ, TS, TS-HI, MBD, FI-MBD) or using the meta-GGA SCAN method, as well as the percentage contribution of the vdW forces on the interaction energies, are investigated and presented in **Table 3**. When comparing the results of the full relaxation using the PBE (GGA) and meta-GGA SCAN methods, we can confirm that the SCAN method take into consideration the vdW forces as interaction energies obtained are larger than those found by PBE calculations (except for the isolated site). Moreover, the meta-GGA SCAN gives interaction energy values very similar to those obtained by dispersion-

corrected PBE methods. This indicates that the meta-GGA SCAN method describes as well accurately the vdW forces.

Table 3. *Water interaction (PBE and dispersion contributions) over selected sites of the silica surface using various dispersion-correction PBE methods and the meta-GGA SCAN method.*

Site		**isolated**	**geminal**	**vicinal**	**Gem-Vic**	**nest-1**	**nest-2**
E_{int} (kJ/mol)	**PBE**	34	29	45	58	56	74
E_{int} (E_{PBE}/E_{disp}) (kJ/mol)	**PBE+D2**	41(36/5)	35(28/7)	60(44/16)	72(58/14)	68(59/9)	97(77/20)
	PBE+D3	42(35/7)	34(29/5)	59(44/15)	69(58/11)	64(57/7)	93(76/17)
	PBE+D3-BJ	42(34/8)	33(29/4)	58(44/14)	71(58/13)	64(58/6)	94(75/19)
	PBE+TS	41(35/6)	33(28/5)	60(44/16)	70(58/12)	65(57/8)	96(74/22)
	PBE+TS-HI	40(35/5)	32(29/3)	54(44/10)	67(57/10)	64(55/9)	88(76/12)
	PBE+MBD	42(34/8)	34(28/6)	58(42/16)	72(57/15)	64(57/7)	95(75/20)
	PBE+FI-MBD	41(36/5)	32(29/3)	56(44/12)	69(58/11)	63(58/5)	93(76/17)
E_{int} (kJ/mol)	**meta-GGA SCAN**	31	43	55	70	71	95
E_{disp}/E_{PBE} (%)	**PBE+D2**	12	20	27	19	13	21
	PBE+D3	17	15	25	16	11	18
	PBE+D3-BJ	19	12	24	18	9	20
	PBE+TS	15	15	27	17	12	23
	PBE+TS-HI	13	9	19	15	14	14
	PBE+MBD	19	18	28	21	11	21
	PBE+FI-MBD	12	9	21	16	8	18

In order to study the interaction types and distances, the FI-MBD corrected-DFT geometry relaxation of the pre-relaxed "fromPBE" system is considered. The initial and final (after relaxation) position of water molecule interacting with the silanols of the amorphous surface defines each selected site, those sites and the water-silanol interaction (expressed in the O-H

bond distances e.g.) types are described in **Table 4**. They are presented in **Figure 3** where the O-H bond distances are revealed. The water-silanols interactions are defined as acceptor or donor H-bonds depending on the site on the silica surface, the number and distances of those H-bonds are interpreted on each site. The H-bond is defined as acceptor when the oxygen atom of the water molecule interacts with a hydrogen atom of the silanol group, while it is defined as donor when the hydrogen atom of water molecule interacts with an oxygen atom of the silanol group of the silica surface. Each site on the silica surface is characterized by a number of H-bonds between water and different types of silanol groups. The length of those H-bonds varies between 1.60 and 2.20 Å depending on the number of H-bonds and the surrounding silanols.

Table 4. *Water-silanol interaction (O-H bonds) types over defined sites of the silica surface.*

Sites	**isolated**	**geminal**	**vicinal**	**Gem-Vic**	**nest-1**	**nest-2**
Initial position of water molecule	**isolated**	**geminal**	**vicinal**	**geminal**	**nest**	**isolated**
Final position of water molecule (after relaxation)	**isolated**	**geminal**	**vicinal**	**vicinal**	**nest**	**nest**
H-bonds	one	2	2	2	4	3
acceptor	one isolated	one geminal	one vicinal	one vicinal	three vicinal	one vicinal & one geminal
donor	-	one geminal	one vicinal	one vicinal	one vicinal	one vicinal

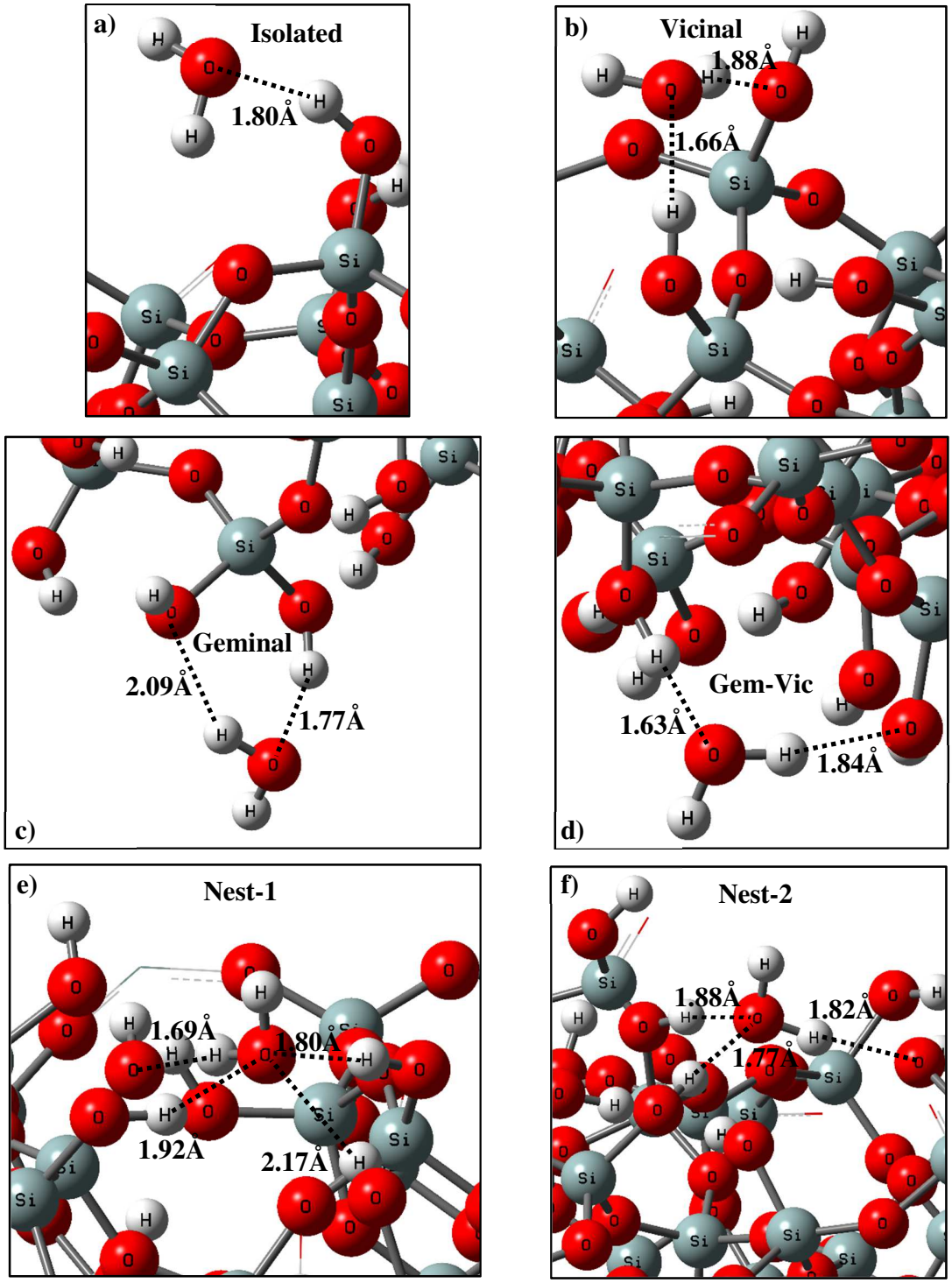

Figure 3. *Water-silanols interaction (O-H bonds) types and distances on various sites of the amorphous silica: a) isolated, b) vicinal, c) geminal, d) Gem-Vic, e) nest-1, and f) nest-2.*

A graphical comparison of the interaction energies computed over the selected sites, using various dispersion-correction methods, is displayed in **Figure 4**. The comparison of the interaction energies over the selected sites of the silica surface shows that water is more likely to adsorb on vicinal silanols than on geminal ones. Water interaction energy for vicinal sites is higher than for geminal sites. This statement is also confirmed on the Gem-Vic site where the water molecule desorbs from its initial position close to the geminal silanol and adsorbs on a neighbor vicinal silanol. This behavior is expected to be related to the effect of steric hindering which affect the formation of H-bonds.

Moreover, it is remarkable that the nest-2 site with three combined geminal-vicinal H-bond interactions shows higher water interaction energy than the nest-1 site with four vicinal H-bond interactions. Among all studied sites, the nest-2 with combined vicinal-geminal H-bond interactions shows the highest interaction energy, about 95 kJ/mol, compared to other sites.

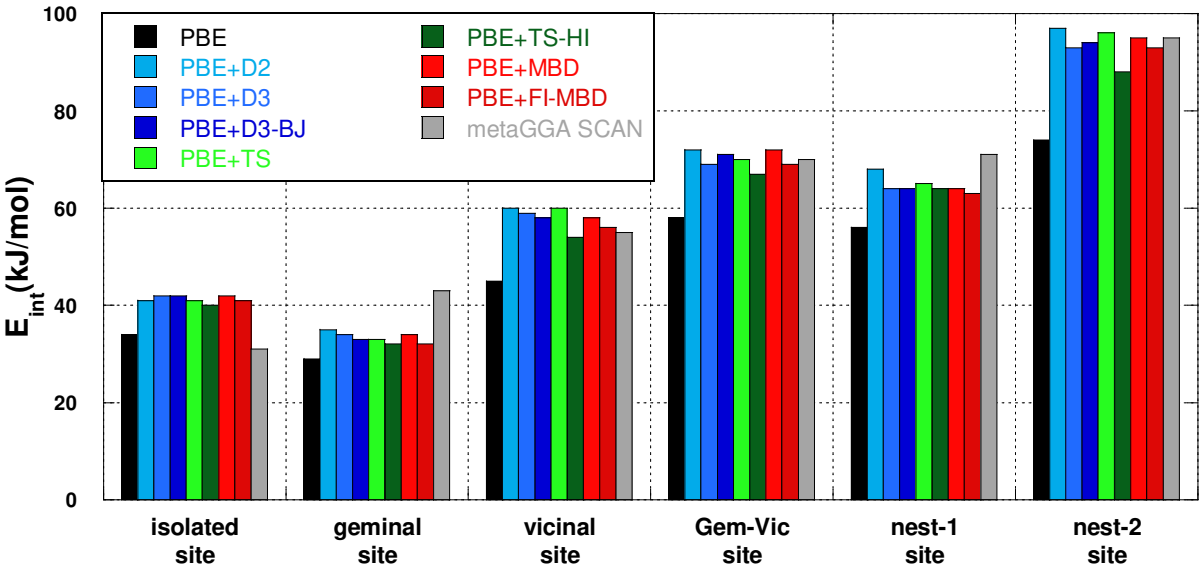

Figure 4. *Water interaction energies over selected sites of the silica surface using various dispersion-correction methods.*

The contribution of the vdW forces on the interaction energy assessed through various dispersion-correction methods are compared in **Figure 5** over various sites of the silica surface. This contribution proved to be important over all studied sites, to reach up to 25% of the interaction energy on the vicinal site. It is clearly seen that on the nest-1 site with four H-bond interactions, the vdW contribution is the lowest comparing to other sites (around 10% depending on the dispersion-correction method). Since the pure electrostatic contributions to the E_{int} is well described in pure DFT (PBE) formalism, and that H-bonds have a strong electrostatic character; one can observe from **Figure 5** that the more H-bonds formed, the higher is the electrostatic contribution and the smaller is the vdW contribution. Therefore, the E_{int} on hydrated silica is indeed electrostatically stabilized while dry/calcined silica surfaces are stabilized through vdW interactions.

The TS-HI method shows the lowest dispersion energy contribution to the interaction energy on most sites, which confirms the underestimation of the interaction energy using this method, as discussed previously.

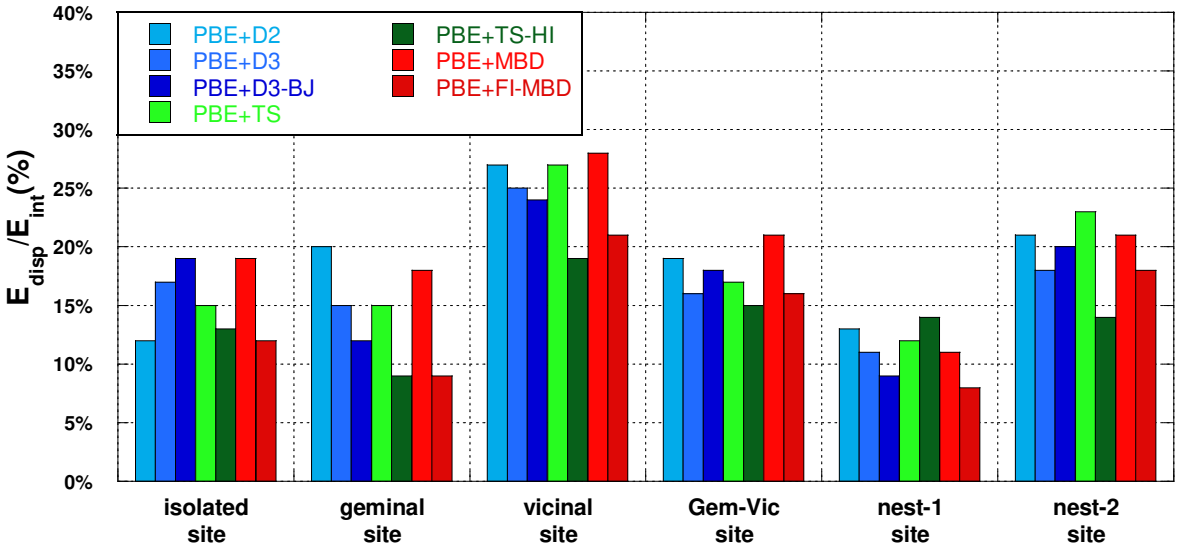

Figure 5. *Percentage contribution of the vdW forces on the interaction energies over the selected sites of the silica surface using different dispersion-correction methods.*

3.3 The effect of water-silanol interactions on the deformation of the silica surface

Table 5 enables to interpret more properly the water interaction energetics on the silica surface, from which we can conclude that the FI-MBD dispersion correction method is the most accurate to relax the pre-relaxed "fromPBE" system. The interaction energy can be affected by two main phenomena, the deformation of the silica surface due to the interaction with the water molecule and the adsorption of the water molecule on the surface. This allows us to decompose the interaction energy in two parts (deformation and adsorption energies, *see equation 3*) in order to interpret the effect of water-silanol interactions on the deformation of the silica surface.

$$E_{int} = E_{ads} + E_{deform} \quad (3)$$

The surface deformation E_{deform} is therefore dependent on the silanol type and the number of H-bonds formed on each site. It can be evaluated as follows:

$$E_{deform} = E_{Sil.slab,clean} + E_{Sil.slab-water} \quad (4)$$

Where $E_{Sil.slab,clean}$ the energy of the clean relaxed silica slab, and $E_{Sil.slab-water}$ the energy of the relaxed hydrated silica slab without the water molecules.

Table 5. *Water-silanol interactions effect on the deformation of the silica surface (FI-MBD-corrected relaxation of the pre-relaxed "fromPBE" configuration).*

Sites		**isolated**	**geminal**	**vicinal**	**Gem-Vic**	**nest-1**	**nest-2**
Energies (kJ/mol)	**Interaction E_{int}**	41	32	56	69	63	93
	Adsorption E_{ads}	46	48	69	78	109	113
	Surface deformation E_{deform}	-5	-16	-13	-9	-46	-20

Silica is known to host water molecules and stabilizes according to its surrounding environment due to its structure flexibility. Indeed, the deformation of the surface until restructuration plays

an important role in the physico-chemical properties of silica [14]. The degree of hydration modulates the surface via the H-bonds formed with the surface silanols. From the surface deformation energies (See **Table 5**) one can observe a trend of relation between the type and number of H-bonds formed and the deformation energy. The largest effect is found for the nest-1 site (-46 kJ/mol), and the smallest effect is found for the isolated silanol involved in only one H-bond. Yet, this reconstruction energy is moderate compared to other systems such as furan or thiophene over MoS_2 (around -200 kJ/mol) [69,70].

3.4 Comparison with crystalline silica surfaces

Historically, amorphous silica models have been elaborated from cuts of crystal structure and contain segments resembling the (100) [71] and (111) β-cristobalite cuts [72], as admitted by Simonetti and coworkers [73,74] when studying the importance of H-bonds interactions during the adsorption of 5-fluorouracil on silica surface. Thus, it would be important to compare the water interaction over the studied amorphous surface with those over various crystalline structures. Three layers of (111), (101) and (001) β-cristobalite surfaces having silanol densities of 4.29, 5.24, and 7.42 OH/nm^2, respectively, are constructed by cutting the bulk geometry of SiO_2 parallel to the (111), (101) and (001) crystallographic planes [75,76]. The two bottom layers are frozen in the geometry of the bulk and the top layer is set free to relax. All silanol groups present at the (111) surface are isolated, those at the (101) surface are vicinal, while those at the (001) surface are geminal. **Figure 6** shows the water interaction configuration on the three β-crystobalite silica surfaces and the H-bonds distances.

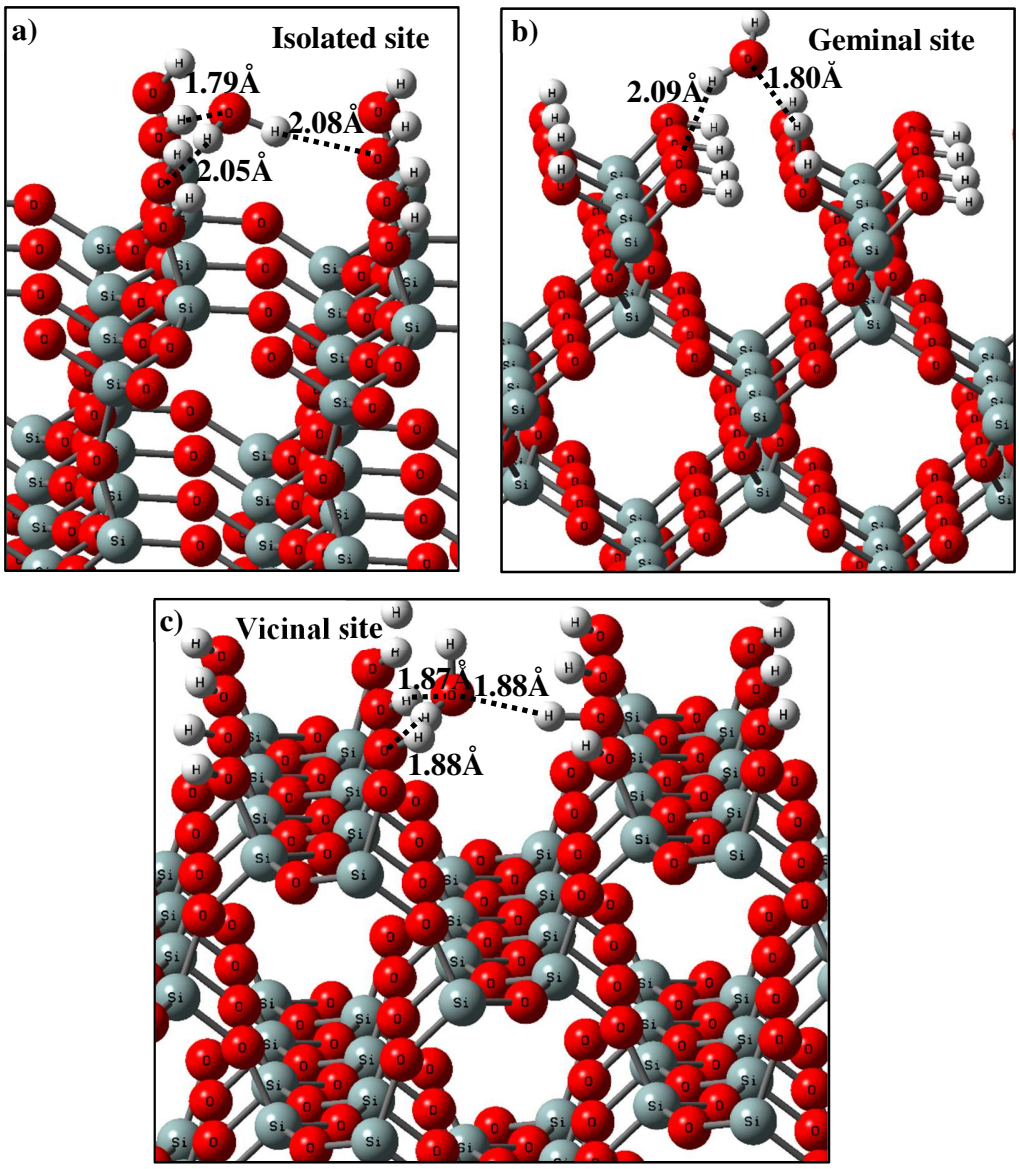

Figure 6. *Water interaction and H-bonds distances on the β-cristobalite silica: a) (111), b) (001), and c) (101) surfaces.*

A comparison of water interaction (PBE and dispersion contribution) energies on the vicinal isolated, and geminal sites of the (101), (111), and (001) β-crystobalite surfaces, respectively, versus "look-alike" sites of the amorphous surface is presented in **Table 6**, and illustrated graphically in **Figure 7**. The interaction energy values of water on amorphous surface admitted for this comparison are those found using FI-MBD-corrected PBE relaxation of "fromPBE"

configuration, as well the same method was used to interpret the water interaction with the crystalline surfaces. Results show that water-silanol interaction on various sites of crystalline surfaces is more exothermic than on "look-alike" sites of the amorphous surface. This can be clearly seen from the vicinal site which shows the highest water interaction energy, while the geminal site shows the lowest on both amorphous and β-cristobalite surfaces. This observation can be very interesting to select an appropriate silica support for separation processes involving water, or for catalytic applications such as hydrodeoxygenation processes in order to decrease the inhibiting effect of water on the adsorption of oxygenated aromatics [77,78].

Table 6. *Comparison of water interaction energies on similar sites of the amorphous and crystalline surfaces (relaxation of "fromPBE" configuration using FI-MBD-corrected PBE calculations).*

Silica surface	**Site**	$\mathbf{E_{int}}$ (kJ/mol)	$\mathbf{E_{PBE}}$ (kJ/mol)	$\mathbf{E_{disp}}$ (kJ/mol)
(101) β-cristobalite	**vicinal**	82	70	12
Amorphous silica	**vicinal**	56	44	12
(111) β-cristobalite	**isolated**	74	61	13
Amorphous silica	**isolated**	41	36	5
(001) β-cristobalite	**geminal**	69	56	13
Amorphous silica	**geminal**	32	29	3

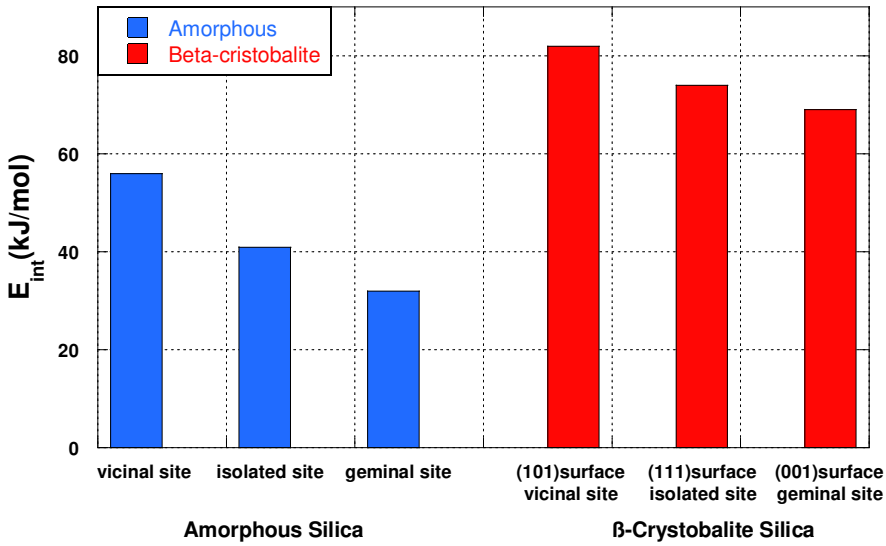

Figure 7. *Comparison between water interaction energies on similar sites of β-cristobalite (111, 101, and 001) vs. amorphous surfaces (relaxation of "fromPBE" configuration using FI-MBD-corrected PBE calculations).*

Figure 7 is of course only a snapshot of the complete picture in which the complete set of silanol groups should be considered in the comparison. A distribution of the silanol geometries per type can unfortunately not be considered due to the geometrical limitations of the model. Nevertheless, the silanols used in this study are chosen to be representative, as is supported by the previous studies undertaken with the same model [21].

4. CONCLUSIONS

Silica-based materials have attracted tremendous interest these recent years in many applications. However, little is known regarding the role of each specific type of surface silanol group. Thus, a molecular description of these silanols and their interaction with water is needed for further improvement of silica formulations. Therefore, DFT calculations (single point and full relaxation) have been performed using different dispersion-correction PBE (PBE + D2, D3, D3-

BJ, TS, TS-HI, MBD, and FI-MBD) and meta-GGA SCAN methods to quantify the water interaction energies with the silica surface in order to distinguish the silanols sites, which allow to tune its properties.

We identified a protocol of calculation, where firstly the system is relaxed using non-corrected PBE method, and then the dispersion-correction relaxations are performed on the pre-relaxed system, in order to reach the correct minima of the potential energy surface. Comparing those correction methods, we found that all of them could be considered reliable when following the supposed protocol of calculation, with a preference for the FI-MBD method for geometrical optimization. Moreover, they all provide very close results, as well does the meta-GGA SCAN method, which strengthen our computed results. However, the TS-HI method provides smaller dispersion energies and thus interaction energies compared to the other dispersion-corrected methods.

We were able to identify the various silanol sites; each of them is characterized by a specific water interaction behavior (number and types of H-bonds) depending on its silanols coverage, types and surrounding environment. This is crucial for understanding the effect of each site on the silica properties and allows suggesting new synthesis methods to control those properties.

Furthermore, the possible deformation of the surface due to the water interaction with the silanol nest proved to be important which need an additional interpretation of the defects generated from applying new synthesis methods. Finally, the comparison of similar sites of amorphous and crystalline surfaces highlighted the fact that the studied amorphous surface is less hydrophilic, which may be promising for catalytic [32,79] or separation [80,81] applications where water can inhibit the adsorption of molecules of interest.

In summary, we discussed the singularity of selected silanol sites of the amorphous surface when interacting with water molecule, the necessity and reliability of dispersion correction methods in DFT calculations, and the effect of water interaction on the silica surface deformation. This study motivates the development of new synthesis of amorphous silica enabling to control the physico-chemical properties of the surface.

Supplementary Material

See Supplementary Material for additional tables S1, S2, S3 and S4 presenting the water-silanols interaction energies (in addition to the PBE and dispersion contributions) over the isolated, geminal, vicinal, and nest-1 sites respectively obtained by single point and geometry relaxation calculations using various dispersion-corrected DFT methods and starting configurations.

Acknowledgements

HPC resources from GENCI-CCRT (Grant 2020- A0080910433) are acknowledged. YB thanks the Lebanese University and the CNRS-Lebanon for funding his Ph.D. We also acknowledge financial support through the PHC CEDRE Future Materials the COMETE project (COnception in silico de Matériaux pour l'EnvironnemenT et l'Energie) co-funded by the European Union under the program "FEDER-FSE Lorraine et Massif des Vosges 2014-2020". Computational resources and services were also provided by the Shared ICT Services Centre funded by the Vrije Universiteit Brussel, the Flemish Supercomputer Center (VSC) and FWO. "FT wishes to acknowledge the VUB for support, among other through a Strategic Research Program awarded to his group.

Conflicts of interest

There are no conflicts of interest to declare.

Data availability

The data that support the findings of this study are available from the corresponding author upon request.

References

[1] D. Brunel, A.C. Blanc, A. Galarneau, F. Fajula, New trends in the design of supported catalysts on mesoporous silicas and their applications in fine chemicals, Catal. Today. 73 (2002) 139–152. https://doi.org/10.1016/S0920-5861(01)00507-7.

[2] Y. Jin, A. Li, S.G. Hazelton, S. Liang, C.L. John, P.D. Selid, D.T. Pierce, J.X. Zhao, Amorphous silica nanohybrids: Synthesis, properties and applications, Coord. Chem. Rev. 253 (2009) 2998–3014. https://doi.org/10.1016/j.ccr.2009.06.005.

[3] L.T. Gibson, Mesosilica materials and organic pollutant adsorption: part A removal from air, Chem Soc Rev. 43 (2014) 5163–5172. https://doi.org/10.1039/C3CS60096C.

[4] H. Li, Y. Niu, Z. Xue, Q. Mu, K. Wang, R. Qu, H. Chen, L. Bai, H. Yang, D. Wei, Adsorption property and mechanism of PAMAM dendrimer/silica gel hybrids for Fe(III) and Ag(I) from N,N-dimethylformamide, J. Mol. Liq. 273 (2019) 305–313. https://doi.org/10.1016/j.molliq.2018.10.039.

[5] F. Naghavi, A. Morsali, M.R. Bozorgmehr, S.A. Beyramabadi, Quantum molecular study of mesoporous silica nanoparticle as a delivery system for troxacitabine anticancer drug, J. Mol. Liq. 310 (2020) 113155. https://doi.org/10.1016/j.molliq.2020.113155.

[6] Y. Berro, S. Gueddida, Y. Bouizi, C. Bellouard, E.-E. Bendeif, A. Gansmuller, A. Celzard, V. Fierro, D. Ihiawakrim, O. Ersen, M. Kassir, F. El Haj Hassan, S. Lebegue, M. Badawi, N. Canilho, A. Pasc, Imprinting isolated single iron atoms onto mesoporous silica by templating with metallosurfactants, J. Colloid Interface Sci. (2020). https://doi.org/10.1016/j.jcis.2020.03.095.

[7] P. Sautet, F. Delbecq, Catalysis and Surface Organometallic Chemistry: A View from Theory and Simulations, Chem. Rev. 110 (2010) 1788–1806. https://doi.org/10.1021/cr900295b.

[8] J. Handzlik, M. Czernecki, A. Shiga, P. Śliwa, Paired interacting orbitals (PIO) study of Mo/SiO2 and Mo/HZSM-5 catalysts for olefin metathesis, Comput. Theor. Chem. 991 (2012) 174–181. https://doi.org/10.1016/j.comptc.2012.04.012.

[9] M.P. Conley, M.F. Delley, F. Núñez-Zarur, A. Comas-Vives, C. Copéret, Heterolytic Activation of C–H Bonds on Cr^{III}–O Surface Sites Is a Key Step in Catalytic Polymerization of Ethylene and Dehydrogenation of Propane, Inorg. Chem. 54 (2015) 5065–5078. https://doi.org/10.1021/ic502696n.

[10] L. Floryan, A.P. Borosy, F. Núñez-Zarur, A. Comas-Vives, C. Copéret, Strain effect and dual initiation pathway in CrIII/SiO2 polymerization catalysts from amorphous periodic models, J. Catal. 346 (2017) 50–56. https://doi.org/10.1016/j.jcat.2016.11.037.

[11] J. Sauer, P. Hobza, R. Zahradnik, Quantum chemical investigation of interaction sites in zeolites and silica, J. Phys. Chem. 84 (1980) 3318–3326. https://doi.org/10.1021/j100461a036.

[12] G.A. Somorjai, Y. Li, Major Successes of Theory-and-Experiment-Combined Studies in Surface Chemistry and Heterogeneous Catalysis, Top. Catal. 53 (2010) 311–325. https://doi.org/10.1007/s11244-010-9449-0.
[13] A. Rimola, M. Fabbiani, M. Sodupe, P. Ugliengo, G. Martra, How Does Silica Catalyze the Amide Bond Formation under Dry Conditions? Role of Specific Surface Silanol Pairs, ACS Catal. 8 (2018) 4558–4568. https://doi.org/10.1021/acscatal.7b03961.
[14] F. Tielens, M. Gierada, J. Handzlik, M. Calatayud, Characterization of amorphous silica based catalysts using DFT computational methods, Catal. Today. (2019). https://doi.org/10.1016/j.cattod.2019.03.062.
[15] A. Douhal, M. Anpo, Chemistry of silica and zeolite-based materials: synthesis, characterization and applications, 1st edition, Elsevier, Waltham, MA, 2019.
[16] J. Sauer, P. Ugliengo, E. Garrone, V.R. Saunders, Theoretical Study of van der Waals Complexes at Surface Sites in Comparison with the Experiment, Chem. Rev. 94 (1994) 2095–2160. https://doi.org/10.1021/cr00031a014.
[17] P. Ugliengo, M. Sodupe, F. Musso, I.J. Bush, R. Orlando, R. Dovesi, Realistic Models of Hydroxylated Amorphous Silica Surfaces and MCM-41 Mesoporous Material Simulated by Large-scale Periodic B3LYP Calculations, Adv. Mater. 20 (2008) 4579–4583. https://doi.org/10.1002/adma.200801489.
[18] B. Coasne, P. Ugliengo, Atomistic Model of Micelle-Templated Mesoporous Silicas: Structural, Morphological, and Adsorption Properties, Langmuir. 28 (2012) 11131–11141. https://doi.org/10.1021/la3022529.
[19] C.S. Ewing, S. Bhavsar, G. Veser, J.J. McCarthy, J.K. Johnson, Accurate Amorphous Silica Surface Models from First-Principles Thermodynamics of Surface Dehydroxylation, Langmuir. 30 (2014) 5133–5141. https://doi.org/10.1021/la500422p.
[20] A. Comas-Vives, Amorphous SiO_2 surface models: energetics of the dehydroxylation process, strain, ab initio atomistic thermodynamics and IR spectroscopic signatures, Phys. Chem. Chem. Phys. 18 (2016) 7475–7482. https://doi.org/10.1039/C6CP00602G.
[21] F. Tielens, C. Gervais, J.F. Lambert, F. Mauri, D. Costa, Ab Initio Study of the Hydroxylated Surface of Amorphous Silica: A Representative Model, Chem. Mater. 20 (2008) 3336–3344. https://doi.org/10.1021/cm8001173.
[22] H. Guesmi, F. Tielens, Chromium Oxide Species Supported on Silica: A Representative Periodic DFT Model, J. Phys. Chem. C. 116 (2012) 994–1001. https://doi.org/10.1021/jp209680r.
[23] J. Handzlik, R. Grybos, F. Tielens, Structure of Monomeric Chromium(VI) Oxide Species Supported on Silica: Periodic and Cluster DFT Studies, J. Phys. Chem. C. 117 (2013) 8138–8149. https://doi.org/10.1021/jp3103035.
[24] Á. Cimas, F. Tielens, M. Sulpizi, M.-P. Gaigeot, D. Costa, The amorphous silica–liquid water interface studied by *ab initio* molecular dynamics (AIMD): local organization in global disorder, J. Phys. Condens. Matter. 26 (2014) 244106. https://doi.org/10.1088/0953-8984/26/24/244106.
[25] M. Pfeiffer-Laplaud, D. Costa, F. Tielens, M.-P. Gaigeot, M. Sulpizi, Bimodal Acidity at the Amorphous Silica/Water Interface, J. Phys. Chem. C. 119 (2015) 27354–27362. https://doi.org/10.1021/acs.jpcc.5b02854.
[26] H. Guesmi, R. Gryboś, J. Handzlik, F. Tielens, Characterization of molybdenum monomeric oxide species supported on hydroxylated silica: a DFT study, Phys Chem Chem Phys. 16 (2014) 18253–18260. https://doi.org/10.1039/C4CP02296C.
[27] D.C. Tranca, A. Wojtaszek-Gurdak, M. Ziolek, F. Tielens, Supported and inserted monomeric niobium oxide species on/in silica: a molecular picture, Phys. Chem. Chem. Phys. 17 (2015) 22402–22411. https://doi.org/10.1039/C5CP03450G.

[28] H. Guesmi, R. Grybos, J. Handzlik, F. Tielens, Characterization of tungsten monomeric oxide species supported on hydroxylated silica; a DFT study, RSC Adv. 6 (2016) 39424–39432. https://doi.org/10.1039/C6RA05395E.
[29] M. Gierada, I. Petit, J. Handzlik, F. Tielens, Hydration in silica based mesoporous materials: a DFT model, Phys. Chem. Chem. Phys. 18 (2016) 32962–32972. https://doi.org/10.1039/C6CP05460A.
[30] N.W. Suek, M.C. Guillaume, J.-Y.P. Delannoy, F. Tielens, Characterization of hydroxylated amorphous silica: a numerical approach, Adsorption. 24 (2018) 267–278. https://doi.org/10.1007/s10450-018-9936-3.
[31] M. Gierada, F. De Proft, M. Sulpizi, F. Tielens, Understanding the Acidic Properties of the Amorphous Hydroxylated Silica Surface, J. Phys. Chem. C. 123 (2019) 17343–17352. https://doi.org/10.1021/acs.jpcc.9b04137.
[32] Y. Berro, S. Gueddida, S. Lebègue, A. Pasc, N. Canilho, M. Kassir, F.E.H. Hassan, M. Badawi, Atomistic description of phenol, CO and H2O adsorption over crystalline and amorphous silica surfaces for hydrodeoxygenation applications, Appl. Surf. Sci. 494 (2019) 721–730. https://doi.org/10.1016/j.apsusc.2019.07.216.
[33] S. Gueddida, M. Badawi, S. Lebègue, Grafting of iron on amorphous silica surfaces from ab initio calculations, J. Chem. Phys. 152 (2020) 214706. https://doi.org/10.1063/5.0007128.
[34] S. Gueddida, S. Lebègue, M. Badawi, Interaction between transition metals (Co, Ni, and Cu) systems and amorphous silica surfaces: A DFT investigation, Appl. Surf. Sci. 533 (2020) 147422. https://doi.org/10.1016/j.apsusc.2020.147422.
[35] M.S. Gordon, J.H. Jensen, Understanding the Hydrogen Bond Using Quantum Chemistry, Acc. Chem. Res. 29 (1996) 536–543. https://doi.org/10.1021/ar9600594.
[36] X. Sun, J. Du, L. Zhao, G. Jiang, Water dissociation and H migration on metal decorated B40: A density functional theory (DFT) study, J. Mol. Liq. 315 (2020) 113759. https://doi.org/10.1016/j.molliq.2020.113759.
[37] T. van der Wijst, C.F. Guerra, M. Swart, F.M. Bickelhaupt, Performance of various density functionals for the hydrogen bonds in DNA base pairs, Chem. Phys. Lett. 426 (2006) 415–421. https://doi.org/10.1016/j.cplett.2006.06.057.
[38] V. Pogorelov, Y. Chernolevska, Y. Vaskivskyi, L.G.M. Pettersson, I. Doroshenko, V. Sablinskas, V. Balevicius, J. Ceponkus, K. Kovaleva, A. Malevich, G. Pitsevich, Structural transformations in bulk and matrix-isolated methanol from measured and computed infrared spectroscopy, J. Mol. Liq. 216 (2016) 53–58. https://doi.org/10.1016/j.molliq.2015.12.099.
[39] L. Goerigk, H. Kruse, S. Grimme, Benchmarking Density Functional Methods against the S66 and S66x8 Datasets for Non-Covalent Interactions, ChemPhysChem. 12 (2011) 3421–3433. https://doi.org/10.1002/cphc.201100826.
[40] K. Burke, The ABC of DFT, Department of Chemistry, University of California, Irvine, CA 92697, 2007.
[41] A. Albavera-Mata, C.M. Zicovich-Wilson, J.L. Gázquez, S.B. Trickey, A. Vela, Long-range exchange limit and dispersion in pure silica zeolites, Theor. Chem. Acc. 137 (2018). https://doi.org/10.1007/s00214-018-2202-7.
[42] M. Fischer, W.J. Kim, M. Badawi, S. Lebègue, Benchmarking the performance of approximate van der Waals methods for the structural and energetic properties of SiO2 and AlPO4 frameworks, J. Chem. Phys. 150 (2019) 094102. https://doi.org/10.1063/1.5085394.
[43] E.P. Hessou, W.G. Kanhounnon, D. Rocca, H. Monnier, C. Vallières, S. Lebègue, M. Badawi, Adsorption of NO, NO2, CO, H2O and CO2 over isolated monovalent cations in faujasite zeolite: a periodic DFT investigation, Theor. Chem. Acc. 137 (2018). https://doi.org/10.1007/s00214-018-2373-2.

[44] S. Grimme, Accurate description of van der Waals complexes by density functional theory including empirical corrections, J. Comput. Chem. 25 (2004) 1463–1473. https://doi.org/10.1002/jcc.20078.
[45] M. Dion, H. Rydberg, E. Schröder, D.C. Langreth, B.I. Lundqvist, Van der Waals Density Functional for General Geometries, Phys. Rev. Lett. 92 (2004) 246401. https://doi.org/10.1103/PhysRevLett.92.246401.
[46] K. Lee, É.D. Murray, L. Kong, B.I. Lundqvist, D.C. Langreth, Higher-accuracy van der Waals density functional, Phys. Rev. B. 82 (2010). https://doi.org/10.1103/PhysRevB.82.081101.
[47] J. Klimeš, D.R. Bowler, A. Michaelides, Van der Waals density functionals applied to solids, Phys. Rev. B. 83 (2011). https://doi.org/10.1103/PhysRevB.83.195131.
[48] U. Zimmerli, M. Parrinello, P. Koumoutsakos, Dispersion corrections to density functionals for water aromatic interactions, J. Chem. Phys. 120 (2004) 2693–2699. https://doi.org/10.1063/1.1637034.
[49] S. Grimme, Semiempirical GGA-type density functional constructed with a long-range dispersion correction, J. Comput. Chem. 27 (2006) 1787–1799. https://doi.org/10.1002/jcc.20495.
[50] T. Bučko, J. Hafner, S. Lebègue, J.G. Ángyán, Improved Description of the Structure of Molecular and Layered Crystals: Ab Initio DFT Calculations with van der Waals Corrections, J. Phys. Chem. A. 114 (2010) 11814–11824. https://doi.org/10.1021/jp106469x.
[51] S. Grimme, J. Antony, S. Ehrlich, H. Krieg, A consistent and accurate ab initio parametrization of density functional dispersion correction (DFT-D) for the 94 elements H-Pu, J. Chem. Phys. 132 (2010) 154104. https://doi.org/10.1063/1.3382344.
[52] S. Grimme, S. Ehrlich, L. Goerigk, Effect of the damping function in dispersion corrected density functional theory, J. Comput. Chem. 32 (2011) 1456–1465. https://doi.org/10.1002/jcc.21759.
[53] A. Tkatchenko, M. Scheffler, Accurate Molecular Van Der Waals Interactions from Ground-State Electron Density and Free-Atom Reference Data, Phys. Rev. Lett. 102 (2009) 073005. https://doi.org/10.1103/PhysRevLett.102.073005.
[54] T. Bučko, S. Lebègue, J. Hafner, J.G. Ángyán, Tkatchenko-Scheffler van der Waals correction method with and without self-consistent screening applied to solids, Phys. Rev. B. 87 (2013) 064110. https://doi.org/10.1103/PhysRevB.87.064110.
[55] T. Bučko, S. Lebègue, J. Hafner, J.G. Ángyán, Improved Density Dependent Correction for the Description of London Dispersion Forces, J. Chem. Theory Comput. 9 (2013) 4293–4299. https://doi.org/10.1021/ct400694h.
[56] T. Bučko, S. Lebègue, J.G. Ángyán, J. Hafner, Extending the applicability of the Tkatchenko-Scheffler dispersion correction via iterative Hirshfeld partitioning, J. Chem. Phys. 141 (2014) 034114. https://doi.org/10.1063/1.4890003.
[57] A. Tkatchenko, R.A. DiStasio, R. Car, M. Scheffler, Accurate and Efficient Method for Many-Body van der Waals Interactions, Phys. Rev. Lett. 108 (2012). https://doi.org/10.1103/PhysRevLett.108.236402.
[58] A. Ambrosetti, A.M. Reilly, R.A. DiStasio, A. Tkatchenko, Long-range correlation energy calculated from coupled atomic response functions, J. Chem. Phys. 140 (2014) 18A508. https://doi.org/10.1063/1.4865104.
[59] T. Bučko, S. Lebègue, T. Gould, J.G. Ángyán, Many-body dispersion corrections for periodic systems: an efficient reciprocal space implementation, J. Phys. Condens. Matter. 28 (2016) 045201. https://doi.org/10.1088/0953-8984/28/4/045201.
[60] T. Gould, S. Lebègue, J.G. Ángyán, T. Bučko, A Fractionally Ionic Approach to Polarizability and van der Waals Many-Body Dispersion Calculations, J. Chem. Theory Comput. 12 (2016) 5920–5930. https://doi.org/10.1021/acs.jctc.6b00925.
[61] J. Sun, R.C. Remsing, Y. Zhang, Z. Sun, A. Ruzsinszky, H. Peng, Z. Yang, A. Paul, U. Waghmare, X. Wu, M.L. Klein, J.P. Perdew, Accurate first-principles structures and energies of diversely bonded

systems from an efficient density functional, Nat. Chem. advance online publication (2016). https://doi.org/10.1038/nchem.2535.
[62] J. Hafner, *Ab-initio* simulations of materials using VASP: Density-functional theory and beyond, J. Comput. Chem. 29 (2008) 2044–2078. https://doi.org/10.1002/jcc.21057.
[63] G. Kresse, J. Hafner, *Ab initio* molecular-dynamics simulation of the liquid-metal–amorphous-semiconductor transition in germanium, Phys. Rev. B. 49 (1994) 14251–14269. https://doi.org/10.1103/PhysRevB.49.14251.
[64] J.P. Perdew, K. Burke, M. Ernzerhof, Generalized Gradient Approximation Made Simple, Phys. Rev. Lett. 77 (1996) 3865–3868. https://doi.org/10.1103/PhysRevLett.77.3865.
[65] G. Kresse, D. Joubert, From ultrasoft pseudopotentials to the projector augmented-wave method, Phys. Rev. B. 59 (1999) 1758–1775. https://doi.org/10.1103/PhysRevB.59.1758.
[66] G. Kresse, J. Furthmüller, Efficient iterative schemes for *ab initio* total-energy calculations using a plane-wave basis set, Phys. Rev. B. 54 (1996) 11169–11186. https://doi.org/10.1103/PhysRevB.54.11169.
[67] M. Chebbi, S. Chibani, J.-F. Paul, L. Cantrel, M. Badawi, Evaluation of volatile iodine trapping in presence of contaminants: A periodic DFT study on cation exchanged-faujasite, Microporous Mesoporous Mater. 239 (2017) 111–122. https://doi.org/10.1016/j.micromeso.2016.09.047.
[68] J. Sun, A. Ruzsinszky, J.P. Perdew, Strongly Constrained and Appropriately Normed Semilocal Density Functional, Phys. Rev. Lett. 115 (2015). https://doi.org/10.1103/PhysRevLett.115.036402.
[69] M. Badawi, S. Cristol, J.-F. Paul, E. Payen, DFT study of furan adsorption over stable molybdenum sulfide catalyst under HDO conditions, Comptes Rendus Chim. 12 (2009) 754–761. https://doi.org/10.1016/j.crci.2008.10.023.
[70] S. Cristol, J. Paul, C. Schovsbo, E. Veilly, E. Payen, DFT study of thiophene adsorption on molybdenum sulfide, J. Catal. 239 (2006) 145–153. https://doi.org/10.1016/j.jcat.2006.01.015.
[71] S. Simonetti, A.D. Compañy, G. Brizuela, A. Juan, β-Cristobalite (001) surface as 4-formaminoantipyrine adsorbent: First principle study of the effect on adsorption of surface modification, Colloids Surf. B Biointerfaces. 148 (2016) 287–292. https://doi.org/10.1016/j.colsurfb.2016.09.006.
[72] A. Juan, D. Damiani, C. Pistonesi, Study of zirconocene and MAO interaction with SiO2 surfaces, Appl. Surf. Sci. 161 (2000) 417–425. https://doi.org/10.1016/S0169-4332(00)00295-6.
[73] S. Simonetti, A.D. Compañy, E. Pronsato, A. Juan, G. Brizuela, A. Lam, Density functional theory based-study of 5-fluorouracil adsorption on β-cristobalite (1 1 1) hydroxylated surface: The importance of H-bonding interactions, Appl. Surf. Sci. 359 (2015) 474–479. https://doi.org/10.1016/j.apsusc.2015.10.147.
[74] A.D. Compañy, A. Juan, G. Brizuela, S. Simonetti, 5-fluorouracil adsorption on hydrated silica: density functional theory based-study, Adsorption. 23 (2017) 321–325. https://doi.org/10.1007/s10450-016-9853-2.
[75] X. Rozanska, F. Delbecq, P. Sautet, Reconstruction and stability of β-cristobalite 001, 101, and 111 surfaces during dehydroxylation, Phys. Chem. Chem. Phys. 12 (2010) 14930. https://doi.org/10.1039/c0cp00287a.
[76] J. Handzlik, J. Ogonowski, Structure of Isolated Molybdenum(VI) and Molybdenum(IV) Oxide Species on Silica: Periodic and Cluster DFT Studies, J. Phys. Chem. C. 116 (2012) 5571–5584. https://doi.org/10.1021/jp207385h.
[77] R. Olcese, M.M. Bettahar, B. Malaman, J. Ghanbaja, L. Tibavizco, D. Petitjean, A. Dufour, Gas-phase hydrodeoxygenation of guaiacol over iron-based catalysts. Effect of gases composition, iron load and supports (silica and activated carbon), Appl. Catal. B Environ. 129 (2013) 528–538. https://doi.org/10.1016/j.apcatb.2012.09.043.

[78] M. Badawi, J.F. Paul, S. Cristol, E. Payen, Y. Romero, F. Richard, S. Brunet, D. Lambert, X. Portier, A. Popov, E. Kondratieva, J.M. Goupil, J. El Fallah, J.P. Gilson, L. Mariey, A. Travert, F. Maug?, Effect of water on the stability of Mo and CoMo hydrodeoxygenation catalysts: A combined experimental and DFT study, J. Catal. 282 (2011) 155–164. https://doi.org/10.1016/j.jcat.2011.06.006.
[79] M. Badawi, J.-F. Paul, S. Cristol, E. Payen, Guaiacol derivatives and inhibiting species adsorption over MoS2 and CoMoS catalysts under HDO conditions: A DFT study, Catal. Commun. 12 (2011) 901–905. https://doi.org/10.1016/j.catcom.2011.02.010.
[80] S. Chibani, M. Chebbi, S. Lebègue, T. Bučko, M. Badawi, A DFT investigation of the adsorption of iodine compounds and water in H-, Na-, Ag-, and Cu- mordenite, J. Chem. Phys. 144 (2016) 244705. https://doi.org/10.1063/1.4954659.
[81] H. Jabraoui, I. Khalil, S. Lebègue, M. Badawi, *Ab initio* screening of cation-exchanged zeolites for biofuel purification, Mol. Syst. Des. Eng. 4 (2019) 882–892. https://doi.org/10.1039/C9ME00015A.